In-Situ Monitoring of Geometric Drift and Thermo-Mechanical Modeling Toward a Digital Twin for Thin-Wall Fused Filament Fabrication

Digambar Killedar[a], Emmanuel Ogunniyi[a,b], Yanzhou Fu[c], Austin Downey[a,d], Lang Yuan[a], and Matthew D. Folsom[e]

[a]Department of Mechanical Engineering, University of South Carolina, Columbia, SC, USA
[b]School of Science and Engineering, Benedict College, Columbia, SC, USA
[c]Department of Ocean and Mechanical Engineering, Florida Atlantic University, Boca Raton, FL, USA
[d]Department of Civil and Environmental Engineering, University of South Carolina, Columbia, SC, USA
[e]Interactive Aptitude LLC, Tyngsboro, MA, USC

ABSTRACT

Additive manufacturing of thin-wall structures by Fused Filament Fabrication (FFF) is highly susceptible to cumulative layer-wise geometric deviations that degrade dimensional accuracy and structural reliability, yet most monitoring approaches emphasize defect detection rather than quantitative tracking of deformation evolution and integration with physics-based models. This study advances progress toward an in-situ digital twin for thin-wall FFF by coupling image-based geometric metrology with layerwise thermo-mechanical finite element analysis (FEA). An L-shaped 1 mm PLA thin wall is fabricated under controlled conditions, while a fixed optical camera captures images after each deposited layer. An OpenCV-based edge-tracking algorithm extracts the visible wall boundary and computes cumulative drift relative to the first layer, generating layer-resolved drift curves and heatmaps that reveal gradual inward bending and a pronounced instability near 20 mm build height. In parallel, a G-code–driven element activation strategy in finite element analysis simulates transient thermal histories and subsequent structural response with thermal strain coupling. Comparison between measured drift and predicted maximum principal strain and stress distributions shows strong correspondence in the critical region where bending and interlayer debonding initiate. By systematically mapping experimental geometric indicators to simulated thermo-mechanical fields, this work establishes a measurement-informed framework for calibrating and updating finite element models. The results demonstrate a practical pathway toward data-informed digital twins capable of interpreting cumulative deformation, identifying instability thresholds, and ultimately enabling closed-loop compensation to improve dimensional fidelity and mechanical performance in thin-wall additive manufacturing.

Keywords: Additive manufacturing; Finite element analysis; model updating; FFF, sensors

1. INTRODUCTION

Additive manufacturing (AM), particularly material extrusion–based processes such as Fused Filament Fabrication (FFF), has transformed the way complex geometries are designed and fabricated across aerospace, biomedical, and structural applications. By depositing material layer by layer, FFF enables rapid prototyping and cost-effective customization while reducing tooling constraints.[1,2] Yet, despite these advantages, dimensional inaccuracy and variability in mechanical performance remain persistent challenges, especially in slender and thin-wall geometries. Thin-wall structures, owing to their low transverse stiffness and open cross-sections, are inherently sensitive to process-induced disturbances. Small thermal gradients, extrusion fluctuations, or

Further author information: (Send correspondence to Austin Downey)
Austin Downey: Email: austindowney@sc.edu

nozzle–part interactions introduced in early layers can accumulate progressively, resulting in geometric drift, interlayer misalignment, and degradation of bonding quality as the build height increases.[3,4] Because even sub-millimeter deviations can significantly alter stress distributions and load transfer paths in thin walls, understanding and predicting the evolution of layer-wise deformation is essential for ensuring structural reliability and dimensional fidelity.[5]

A growing body of research has focused on in-situ monitoring strategies to address these challenges. Reviews of FFF monitoring systems highlight the use of thermal sensing, vibration analysis, acoustic emission, electrical feedback, and vision-based imaging to detect process instabilities during fabrication.[6] Among these, camera-based approaches are particularly attractive because they are non-contact, cost-effective, and capable of capturing rich spatial information over large regions of interest.[7] Prior work has demonstrated defect detection, anomaly classification, and surface quality assessment using both classical computer vision techniques and deep learning frameworks.[8,9] However, most existing studies emphasize binary defect identification, determining whether a failure has occurred rather than quantifying the continuous, layer-wise geometric evolution that precedes visible failure. For thin-wall FFF structures, where deformation accumulates gradually and may culminate in bending or debonding at a critical height, this distinction is crucial. Quantitative tracking of wall edge drift and geometric deviation throughout the build can reveal the onset and growth of thermo-mechanical instability long before catastrophic failure becomes evident.

Within this context, the concept of a digital twin offers a compelling pathway forward.[10] A digital twin of an FFF process should not only replicate nominal deposition parameters but also evolve in response to measured geometric deviations and thermal histories. For thin-wall structures, such a twin must capture the coupling between cumulative edge drift, layerwise thermal shrinkage, and stress development. However, most current digital representations remain open-loop: simulations are performed using prescribed parameters, and experimental measurements are used only for post hoc comparison. The opportunity lies in establishing measurement-rich frameworks that enable systematic comparison between observed geometric drift and finite element predictions, thereby laying the foundation for future model updating and closed-loop compensation strategies.

In this work, an in-situ, imaging-based geometric monitoring framework for thin-wall FFF structures is presented, which directly compares the measured layerwise wall drift with thermo-mechanical finite element simulations. An L-shaped thin PLA wall is fabricated under controlled printing conditions, and a fixed optical setup captures an image after each deposited layer. Using an OpenCV-based edge detection algorithm, the visible wall edge is extracted and referenced to the first printed layer, enabling quantitative measurement of cumulative drift as a function of build height. The resulting drift heat maps and mean layerwise displacement curves provide a high-resolution view of geometric evolution throughout the print. In parallel, a layer-by-layer thermo-mechanical Finite element model (FEM) is developed using element activation driven by the actual printing sequence, incorporating transient thermal analysis followed by structural analysis with thermal strain coupling.[11,12] The FEM are used to validate the anomalies observed during the process, and they give a better understanding of what's happening at the micro level at the layers. By comparing experimental drift patterns with simulated strain and stress distributions, particularly the emergence of elevated principal strains near critical build heights, we establish correspondence between observed bending and predicted thermo-mechanical response.

Although the present study does not yet implement real-time control or automated parameter updating, it demonstrates a critical step toward physics-based digital twins[13] for thin-wall additive manufacturing. The integration of camera-based geometric metrology with layerwise FEA provides a physics-grounded framework for interpreting cumulative deviation, identifying instability thresholds, and calibrating simulation parameters against measured behavior. The key contributions of this work are: (i) develops a low-cost, in-situ vision-based method to quantify layer-wise geometric drift in thin-wall FFF printing; (ii) integrates image-based measurements with a G-code–driven thermo-mechanical finite element model to establish a physics-informed digital twin, and (iii) demonstrates how experimental drift data can be used to calibrate and update simulations, enabling future data-driven[14] and closed-loop[15,16] control of additive manufacturing processes.

2. BACKGROUND STUDIES

In-situ monitoring in fused filament fabrication (FFF) has gained significant attention due to the process sensitivity of thermoplastic deposition and the need to improve repeatability and part reliability.[17] Unlike post-process inspection, in-situ approaches aim to detect instabilities during fabrication, enabling early intervention and reducing part rejection. Various sensing modalities have been investigated, including thermal sensing,[18] encoder-based kinematic feedback, force/torque sensing, vibration and acoustic emission,[17] electrical monitoring, and vision-based imaging.[19] These techniques target process anomalies such as extrusion defects, nozzle clogging, layer shifting, warpage, and dimensional drift. Although many laboratory-scale systems have been demonstrated, widespread industrial adoption remains limited by challenges in calibration, synchronization, and development of robust, generalizable decision frameworks across materials and geometries.[6,20]

Vision-based monitoring is widely used in FFF because cameras are low-cost, non-contact, and provide rich spatial information. Images are typically captured from side, top, or multi-view configurations and processed to assess print quality or detect abnormal patterns.[21] Early approaches relied on classical computer vision techniques such as edge detection, thresholding, and template matching. More recent methods employ deep learning for defect classification, object detection, and semantic segmentation, often enabling near real-time performance.[8] However, these methods typically require extensive labeled datasets and may struggle to generalize across materials, geometries, and printers. Transfer learning and foundation models have been proposed to improve adaptability under limited supervision.[9] Despite these advances, most vision-based studies focus on discrete defect detection rather than quantitative, layer-wise geometric measurement. For thin-wall structures, where small deviations accumulate progressively, continuous tracking of geometric drift is essential for understanding instability development and informing physics-based digital twin models.

Dimensional accuracy in FFF is governed by machine kinematics, extrusion stability, thermal shrinkage, and structural stiffness. Process parameters such as temperature, speed, layer height, raster strategy, and cooling conditions significantly influence both global dimensional error and local geometric artifacts.[22] Errors may be systematic or stochastic, highlighting the need for measurement approaches capable of resolving deviations at multiple scales. Conventional geometric assessment relies on post-process metrology tools such as calipers, coordinate measuring machines (CMM), 3D scanning, and profilometry. While accurate, these methods do not capture the evolution of deviations during printing. In-situ geometric measurement addresses this limitation by extracting features such as contour deviation, wall thickness, centerline drift, and layer offset directly from process data. Camera-based approaches are particularly effective when supported by proper calibration, controlled lighting, and a consistent region of interest. For thin-wall structures, tracking the wall edge across layers provides a practical measure of cumulative geometric drift with build height, enabling direct comparison with design intent and physics-based finite element predictions.

Finite element analysis (FEA) is widely used to model the thermal and thermo-mechanical behavior of FFF, including temperature evolution, residual stresses, warpage, and distortion. Layer-by-layer simulation is typically implemented using element activation, where elements are sequentially "born" according to the deposition schedule, capturing the evolving stiffness and thermal boundary conditions during printing.[11] A major challenge in FFF simulation is computational cost, as resolving steep thermal gradients near the moving nozzle requires fine meshes and small time steps. To improve efficiency, recent studies have explored hybrid activation schemes, adaptive discretization, and reduced-order thermal models.[12] Linking element activation directly to G-code further enhances realism by synchronizing the simulation with the actual toolpath, improving agreement between predicted and measured deformation.[23] For thin-wall structures, thermo-mechanical modeling is particularly important because low stiffness amplifies thermal contraction effects and residual stresses, leading to geometric drift and instability. However, model accuracy depends strongly on temperature-dependent material properties, heat transfer assumptions, and representation of interlayer bonding, which are critical for developing credible digital twins.

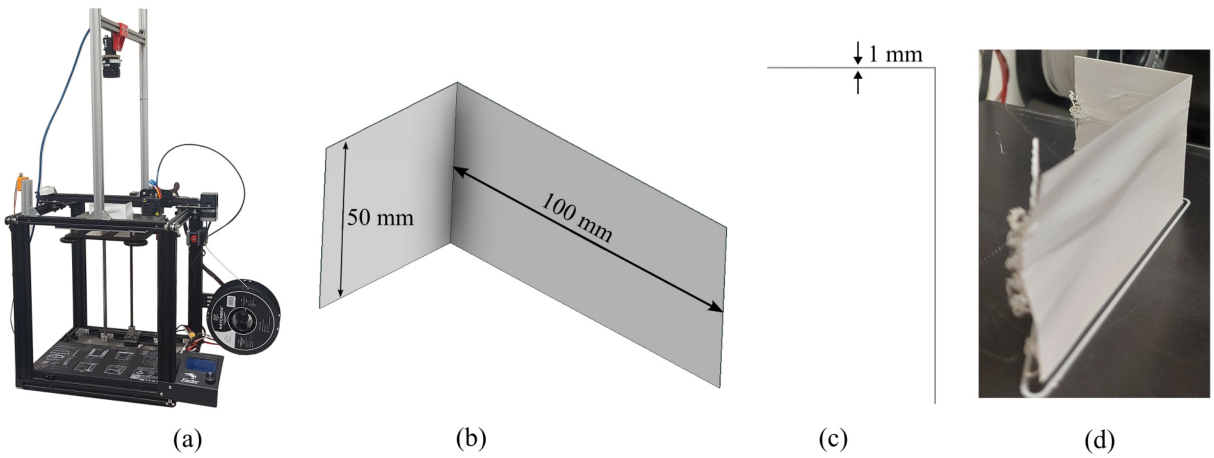

Figure 1: Details of thin wall design, showing: (a) experimental setup; (b) design of L-wall, and (c) top view of 1 mm thick L-wall (d) actual printed L-wall.

3. METHODOLOGY

This section explains the experimental procedure, the finite element analysis, and the edge detection process.

3.1 Experimental Setup

All specimens in this study were fabricated using a Creality Ender-5 Fused Filament Fabrication (FFF) printer. A standard thermoplastic filament of PLA with a nominal diameter of 1.75 mm was used. The printer was equipped with a brass nozzle of diameter 0.2 mm. Printing parameters were selected based on preliminary trials to ensure stable deposition. The bed temperature is maintained at 60°C and the nozzle temperature at 220°C. The speed of the moving nozzle is set at 60% of maximum speed. These key parameters were kept constant throughout the experiments to isolate the effects of cumulative geometric deviation.

Thin-wall specimens were designed to amplify sensitivity to geometric deviation and interlayer bonding variability, and are printed to maximize the deformations and warping during the printing process. Open cross sections are more prone to warping due to external load as compared to the closed sections.

Figure 1(a) shows the Ender-5 machine used for printing this thin L-section, while Figure 1(b) and (c) show the printed wall geometry. Figure 1(d) shows the actual printed thin L-section during this study. Images and videos of layer printing are captured with an industrial optical camera (model BFS-U3-200S6M-C manufactured by FLIR) attached to the printer and a fixed focal length lens(model LH50HC manufactured by Kowa).

The images captured while printing are fed to the Python program utilizing the OpenCV computer vision library for further post-processing. The OpenCV program identifies the first printed layer and assigns a reference green line to the initially printed layer. This acts as a standard location for benchmarking the further printed layers. As the printing progresses, the program identifies the newly printed edge and compares its location with the baseline green line. Using this approach, the drift in the wall is identified as the printing proceeds layer by layer. This drift at the edge of the thin wall is compared with test and FEA results.

3.2 Finite Element Analysis and Edge Detection

Figure 2 shows the flowchart for the overall steps of the FEA workflow. This G-code file of the sliced part is modified to only include the G-code related to printing of the layers and not any other machine parameters. Then the G-code is imported into ANSYS Workbench. The L-wall is discretized in such a way that it mimics the

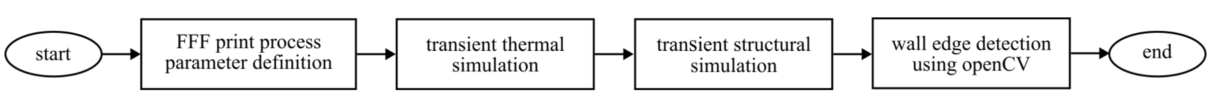

Figure 2: FEA process flow chart.

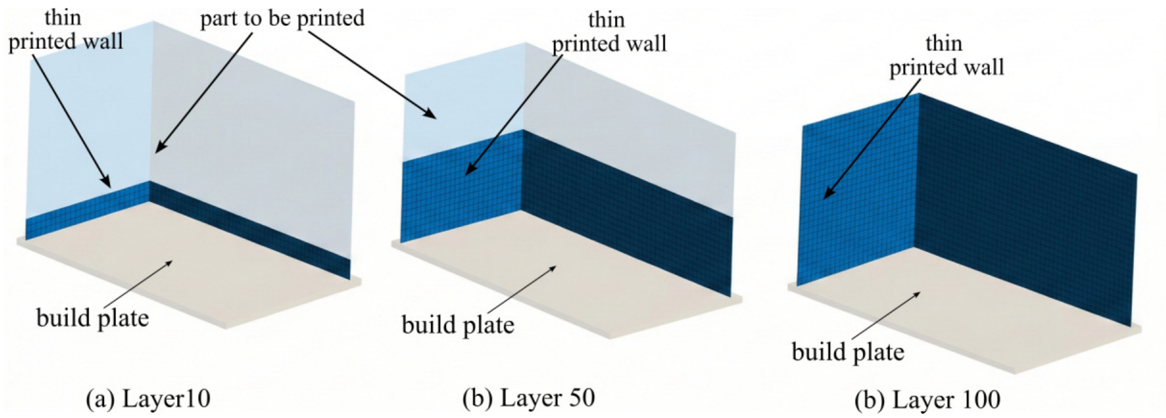

Figure 3: Layer by layer element activation during FFF.

layer and piecewise printing in the ANSYS additive manufacturing environment. The cluster volume is defined, which essentially controls the number of elements for which the 'birth' and 'death' commands are applied during printing in multiple load steps. The other parameters, which were defined on the machine, are also used in the analysis setting for FFF printing in ANSYS Workbench. The Feed rate, bed temperature, nozzle temperature, and cooling time after the printing is completed are the necessary initial conditions required to be defined in the additive module.

The next step is to define the transient thermal framework that prints each clustered element at each time step at the defined process/nozzle temperature. This simulation step gets completed after printing all the elements or clusters of the thin wall. Figure 3 shows a few of the clusters created for simulation during printing. During the printing of the full L-wall, the thermal histories are recorded throughout the process. These thermal histories are then given as boundary and initial conditions to the structural module. During structural simulations, the same clusters and printing strategy were implemented along with respective thermal histories imported as thermal conditions at the same time stamps. This gives rise to deformation and stresses due to temperature. The values of stress and strains are recorded at all time steps of the simulation. Generally, it is recommended to run the structural simulation with the NLGEOM feature switched on, so that thermal deformations can be captured accurately.

4. RESULTS AND DISCUSSION

This section presents the experimental and simulation results, including edge detection, drift heatmaps, mean drift analysis, and finite element modeling outcomes.

4.1 Edge Detection and Bending of Thin Walls

The thin-wall structures are monitored in-situ to quantify deformation mechanisms such as bending and interlayer debonding. Due to its small thickness (1 mm) and open L-shaped cross-section, the wall has low transverse stiffness, making it highly sensitive to thermo-mechanical effects during layer-by-layer deposition. As the build height increases, cumulative thermal shrinkage induces inward bending. An edge detection algorithm is used to measure this geometric deviation. In the processed images, the red line represents the detected wall edge, while the green line represents the nominal (ideal) straight wall location. The deviation between these two lines provides a quantitative measure of wall drift. Figure 4(a) and (b) illustrate the edge detection procedure, where Figure 4(a) indicates no deviation, and Figure 4(b) shows thin-wall deviation during printing and simulation in a pictorial way. During actual printing of the thin wall layer, overlap can be seen in Figure 4(c) between the green line and the actual printed white colored layer, and the white printed layer starts moving to the left of the green line as indicated in Figure 4(d) near layer 50.

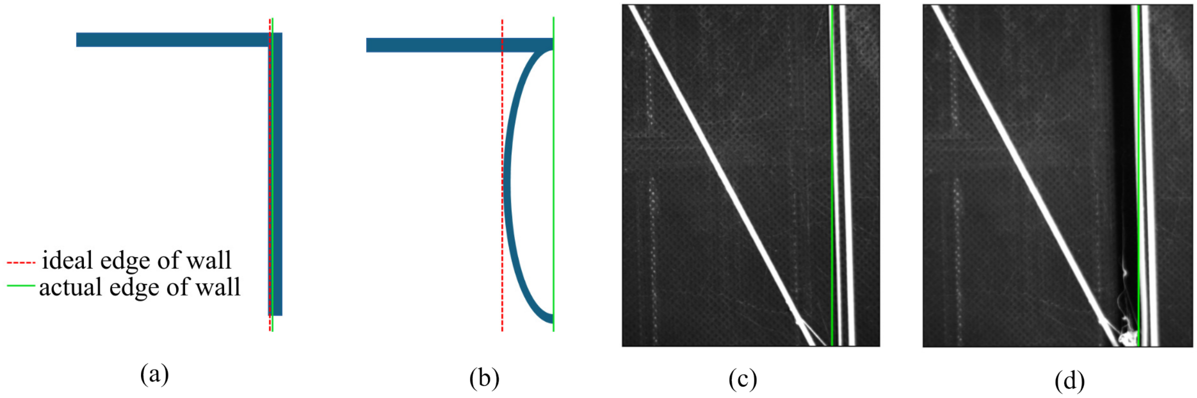

Figure 4: Edge detection and edge printing prediction using OpenCV (a) layer-1; (b) layer with wall bending; (c) layer-1, and; (d) layer-50.

Analysis of successive layers shows that the detected edge remains close to the nominal line in the early stages of printing, but progressively deviates as height increases. This layer-wise deviation, referred to as edge drift, reflects cumulative geometric error. The primary driver is asymmetric cooling of the deposited material, which generates differential shrinkage and bending. The resulting lateral deflection grows with each additional layer. These measured drift patterns serve as experimental inputs for validating and updating the thermo-mechanical finite element model. By directly comparing observed bending with predicted strain and stress distributions, the framework supports the development of a data-informed digital twin for thin-wall FFF structures.

Figure 5 presents the cumulative edge drift of the L-shaped thin PLA wall over 100 printed layers. The x-axis represents layer number (1–100), and the y-axis represents wall height (0–50 mm). Each color value indicates the displacement of the tracked inner wall edge relative to the reference layer (layer 1), measured in pixels. Positive values correspond to inward wall movement, while negative values indicate outward movement. Because all layers are referenced to the same baseline, the map represents cumulative drift rather than incremental layer-to-layer variation. This representation makes it possible to identify whether deformation develops gradually or appears as sudden instability events. Distinct vertical bands in Figure 5 indicate layer-wide changes affecting most of the wall height, while localized patches reflect height-dependent behavior. A prominent vertical band appears around layers 45–50, spanning nearly the full wall height. This feature indicates a global geometric shift rather than a local fluctuation. The corresponding build height (approximately 20–25 mm) aligns with the region where bending becomes visually evident. Such behavior suggests the onset of thermo-mechanical instability.

Additional localized regions of drift are observed around layers 20, 64–73, and 83–90, indicating that deformation is not uniform along the height. The lower wall region (0–10 mm) exhibits higher variability in early layers. This behavior is likely influenced by optical effects near the build plate rather than structural instability,

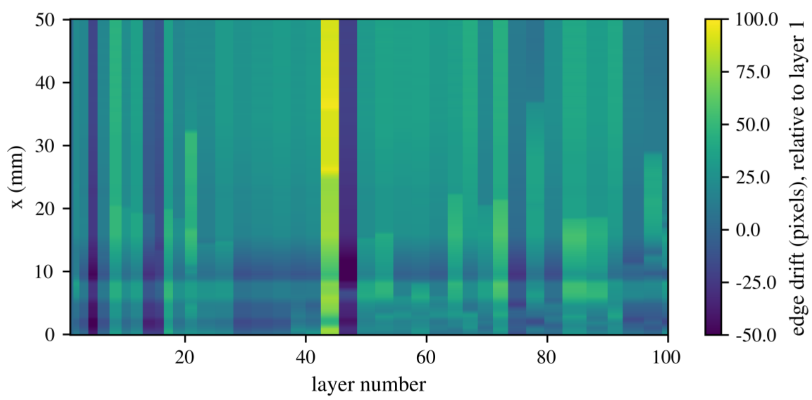

Figure 5: Drift heatmap: x-axis is layer, y-axis is height of the layer from the bottom.

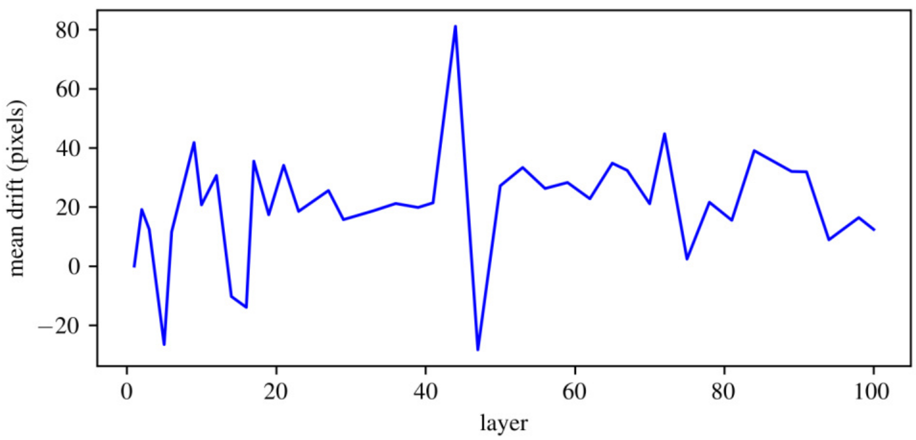

Figure 6: Mean edge drift vs layer.

since the base remains mechanically constrained. The overall green-to-yellow bias in the heatmap indicates a dominant inward drift as printing progresses. The magnitude range (approximately –55 to +100 pixels) shows larger positive excursions, consistent with inward bending caused by asymmetric cooling and thermal shrinkage. Although some negative values may arise from edge detection uncertainty, the dominant trend reflects cumulative thermo-mechanical deformation in one direction.

The mean drift per layer is shown in Figure 6. This metric represents the average lateral displacement of the wall edge, relative to the reference layer (layer 1), computed along the full height of the wall for each printed layer. By averaging the measured edge drift at multiple points, a single scalar value is obtained per layer.

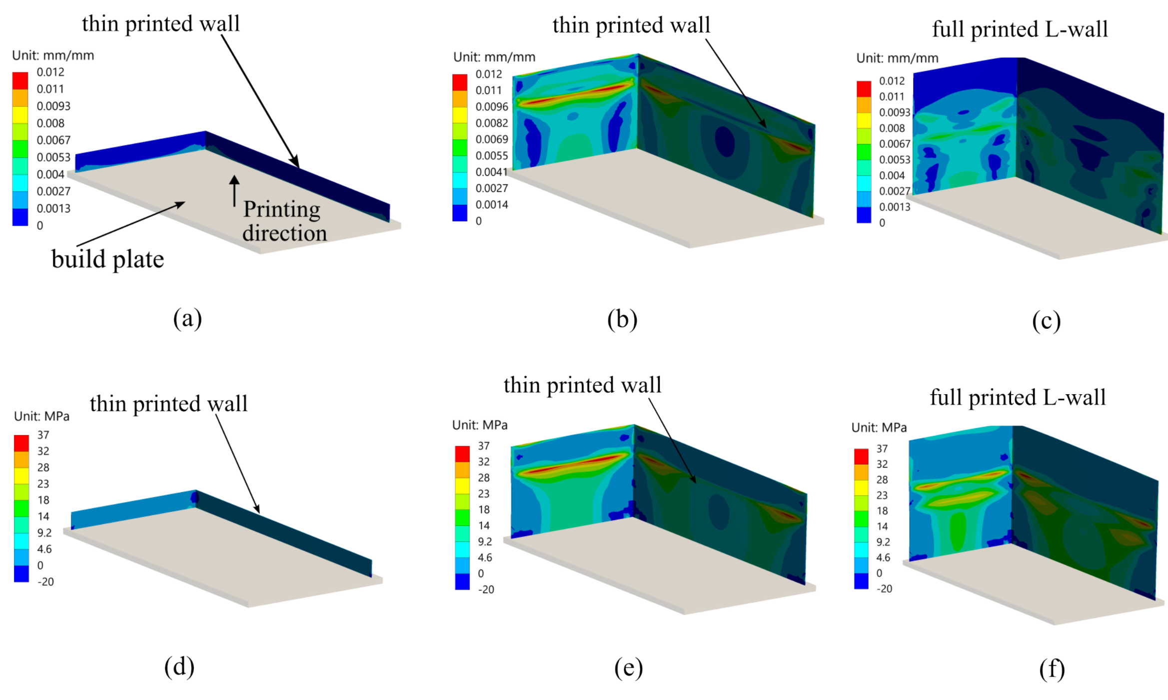

Figure 7: FEA results: (a)maximum principal elastic strain at layer 10; (b) maximum principal elastic strain at layer 50; (c) maximum principal elastic strain in L wall; (d) maximum principal stress at layer 10; (e) maximum principal stress at layer 50, and; (f) maximum principal stress in L wall.

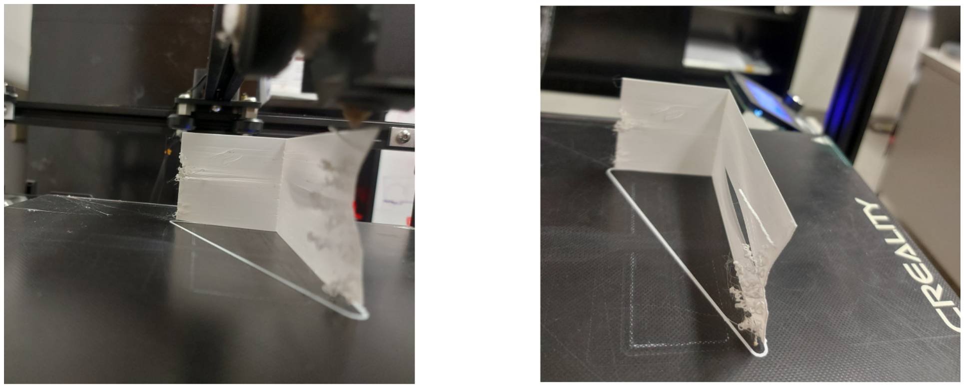

(a) (b)

Figure 8: Actual defect observed in thin wall printing, showing: (a) maximum drifting and observed bending, and; (b) Debonding due to excessive bending.

4.2 Finite Element Analysis Calibration

A layer-by-layer thermo-mechanical finite element simulation was performed to replicate the printing process and predict the evolution of strain and stress in the thin wall. The results are shown in Figure 7(a)–(f). As the build progresses, the simulation predicts a concentration of maximum principal elastic strain near a height of approximately 20 mm. This region corresponds closely to the instability zone identified in the drift heatmap and the mean drift curve. For PLA material, the maximum principal stress is a relevant indicator because tensile stresses dominate crack initiation and interlayer failure. The FEA results show elevated tensile principal stresses in the same region where high strains develop, indicating a thermo-mechanical mechanism driving bending and potential damage.

Experimental observations support these predictions. As shown in Figure 8, significant inward bending occurs near the same height (20mm), followed by interlayer debonding. The agreement between measured geometric drift and predicted strain/stress concentration demonstrates that the finite element model captures the dominant deformation mechanism responsible for instability. Although the current simulation uses a linear elastic material model and does not explicitly include fracture or cohesive debonding behavior, it successfully identifies the critical height and stress state associated with failure initiation.

5. CONCLUSION

This paper presented a measurement-informed framework for advancing in-situ digital twins of thin-wall structures fabricated by fused filament fabrication (FFF). Using an L-shaped 1 mm PLA wall, the study addressed cumulative layer-wise geometric deviation, a key source of dimensional inaccuracy and instability in slender geometries. Rather than focusing solely on defect detection, the work quantitatively tracked deformation evolution and linked measurements to a physics-based finite element model. An in-situ vision system measured cumulative edge drift relative to the first layer using OpenCV-based detection, generating drift heatmaps and mean drift curves that revealed progressive inward bending and a clear instability near 20 mm build height. A G-code–driven thermo-mechanical finite element model with layer-by-layer element activation simulated thermal histories and structural response, predicting concentrated maximum principal strain and tensile stress in the same critical region.

The strong agreement between measured drift and predicted strain/stress fields confirms that the model captures the dominant thermo-mechanical mechanism driving instability. Although limited to linear elastic behavior without explicit fracture modeling, the simulation successfully identified the onset and location of failure initiation, providing a basis for model calibration and updating. The study demonstrates how image-based geometric metrics can serve as physically meaningful observables for digital twin development. By linking experimental deformation to simulated thermo-mechanical fields, it advances the transition from open-loop simulation toward data-informed digital twins for thin-wall FFF structures, with future work aimed at incorporating damage modeling and real-time model updating.

6. ACKNOWLEDGMENTS

This research was supported by the United States' National Science Foundation (NSF), USA, Grants Nos. CCF-2503055, and CPS-2237696. This work is also partially supported by the National Institute of Standards & Technology, United States, under grant number 70NANB23H030, as well as the South Carolina Space Grant Consortium under grants 21-117-RID RGP-SC-009, 25-073-REAP-SC-001, and 25-073-BTC-SC-001. Additional support is provided by the United States' National Science Foundation (NSF) through the NSF ASEE Fellowship. Any opinions, findings, conclusions, or recommendations expressed in this material are those of the authors and do not necessarily reflect the views of the National Science Foundation, the South Carolina Space Grant Consortium, or the National Institute of Standards & Technology.

REFERENCES

[1] Singh, S., Singh, G., Prakash, C., and Ramakrishna, S., "Current status and future directions of fused filament fabrication," *Journal of Manufacturing Processes* **55**, 288–306 (2020).

[2] Yadav, A., Rohru, P., Babbar, A., Kumar, R., Ranjan, N., Chohan, J. S., Kumar, R., and Gupta, M., "Fused filament fabrication: A state-of-the-art review of the technology, materials, properties and defects," *International Journal on Interactive Design and Manufacturing (IJIDeM)* **17**(6), 2867–2889 (2023).

[3] Wang, K., Liu, Y., Wang, J., Xiang, J., Yao, S., and Peng, Y., "On crashworthiness behaviors of 3D printed multi-cell filled thin-walled structures," *Engineering Structures* **254**, 113907 (2022).

[4] Wolfs, R. and Suiker, A., "Structural failure during extrusion-based 3D printing processes," *The International Journal of Advanced Manufacturing Technology* **104**(1), 565–584 (2019).

[5] Ding, J., Qu, S., Zhang, L., Wang, M. Y., and Song, X., "Geometric deviation and compensation for thin-walled shell lattice structures fabricated by high precision laser powder bed fusion," *Additive Manufacturing* **58**, 103061 (2022).

[6] Fu, Y., Downey, A., Yuan, L., Pratt, A., and Balogun, Y., "In situ monitoring for fused filament fabrication process: A review," *Additive Manufacturing* **38**, 101749 (Feb. 2021).

[7] Chen, Z., Santhakumar, P., Granland, K., Troeung, C., Chen, C., and Tang, Y., "Predicting future warping from the first layer: A vision-based deep learning method for 3D printing monitoring," in [*2023 IEEE 19th international conference on automation science and engineering (CASE)*], 1–6, IEEE (2023).

[8] Werkle, K. T., Trage, C., Wolf, J., and Möhring, H.-C., "Generalizable process monitoring for FFF 3D printing with machine vision," *Production Engineering* **18**(3), 593–601 (2024).

[9] Deng, X., Tian, H., Wang, Z., Xiao, F., Qiao, J., and Li, L., "In-situ real-time defect detection, mitigation and self-supervised adaptation based on visual foundation model for material extrusion additive manufacturing," *Additive Manufacturing* **111**, 104978 (2025).

[10] Zolfagharian, A., Jin, L., Ge, Q., Liao, W., Díaz Lantada, A., Franco Martínez, F., Zhang, T., Liu, T., Wang, C. C. L., Mosallanejad, M. H., Ghanavati, R., Saboori, A., De Blas De Miguel, A., Solórzano-Requejo, W., Cai, Y., Dong, X., Qu, H., Samadiani, N., Huang, G., Downey, A., Fu, Y., Yuan, L., Lee, T. G., Baniya, A. A., Waseem, E., Sani, A. R., Kouzani, A. Z., Wu, Y., Nemitz, M. P., Shirzad, M., Oh, D., Nam, S. Y., Bonatti, A. F., Chiesa, I., Fortunato, G. M., Vozzi, G., De Maria, C., and Bodaghi, M., "Roadmap on artificial intelligence-augmented additive manufacturing," *Advanced Intelligent Systems* (Jan. 2026).

[11] Behseresht, S., Park, Y. H., Love, A., and Valdez Pastrana, O. A., "Application of numerical modeling and finite element analysis in fused filament fabrication: A review," *Materials* **17**(17), 4185 (2024).

[12] Ramos, M., Mittermeier, T., and Kiendl, J., "Efficient simulation of the heat transfer in fused filament fabrication by a layerwise state-space method," *Journal of Manufacturing Processes* **94**, 550–563 (May 2023).

[13] Fu, Y., Downey, A. R., Yuan, L., Huang, H.-T., and Ogunniyi, E. A., "Simulation-in-the-loop additive manufacturing for real-time structural validation and digital twin development," *Additive Manufacturing* **98**, 104631 (Jan. 2025).

[14] Fu, Y., Downey, A. R., Yuan, L., and Huang, H.-T., "Real-time structural validation for material extrusion additive manufacturing," *Additive Manufacturing* **65**, 103409 (Mar. 2023).

[15] Chen, Y.-P., Karkaria, V., Tsai, Y.-K., Rolark, F., Quispe, D., Gao, R. X., Cao, J., and Chen, W., "Real-time decision-making for digital twin in additive manufacturing with model predictive control using time-series deep neural networks," *Journal of Manufacturing Systems* **80**, 412–424 (June 2025).

[16] Fan, H., Liu, C., Bian, S., Ma, C., Huang, J., Liu, X., Doyle, M., Lu, T., Chow, E., Chen, L., Fuh, J. Y. H., Lu, W. F., and Li, B., "New era towards autonomous additive manufacturing: a review of recent trends and future perspectives," *International Journal of Extreme Manufacturing* **7**, 032006 (Jan. 2025).

[17] Li, Y., Zhao, W., Li, Q., Wang, T., and Wang, G., "In-situ monitoring and diagnosing for fused filament fabrication process based on vibration sensors," *Sensors* **19**(11), 2589 (2019).

[18] Lewis, J., Moore, A. L., et al., "In situ infrared temperature sensing for real-time defect detection in additive manufacturing," *Additive Manufacturing* **47**, 102328 (2021).

[19] Cunha, F. G., Santos, T. G., and Xavier, J., "In situ monitoring of additive manufacturing using digital image correlation: a review," *Materials* **14**(6), 1511 (2021).

[20] Oleff, A., Küster, B., Stonis, M., and Overmeyer, L., "Process monitoring for material extrusion additive manufacturing: a state-of-the-art review," *Progress in Additive Manufacturing* **6** (Dec. 2021).

[21] Holzmond, O. and Li, X., "In situ real time defect detection of 3D printed parts," *Additive manufacturing* **17**, 135–142 (2017).

[22] Equbal, A., Murmu, R., Kumar, V., and Equbal, M. A., "A recent review on advancements in dimensional accuracy in fused deposition modeling FDM 3D printing," *AIMS Materials Science* **11**, 950–990 (Oct. 2024).

[23] Farh, M. M. and Gribniak, V., "Thermo-mechanical approach to material extrusion process during fused filament fabrication of polymeric samples," *Materials* **18**, 4537 (Sept. 2025).